International Journal of Multiphase Flow 34 (2008) 924–930

Contents lists available at ScienceDirect

International Journal of Multiphase Flow

journal homepage: www.elsevier.com/locate/ijmulflow

Experimental investigation of interparticle collision in the upper dilute zone of a cold CFB riser

Xuecheng Wu, Qinhui Wang *, Zhongyang Luo, Mengxiang Fang, Kefa Cen

State Key Laboratory of Clean Energy Utilization, Zhejiang University, Hangzhou 310027, P.R. China

ARTICLE INFO

Article history:
Received 2 July 2007
Received in revised form 11 April 2008
Available online 8 May 2008

Keywords:
Interparticle collision
CFBs
Gas–solid two-phase flow
High-speed imaging system

ABSTRACT

Interparticle collision plays an important role in the mechanics of gas–solid two-phase flows. The paper presents direct measurements of collision rate as well as collision properties of spherical glass beads with sizes of 500 ± 50 μm in the upper dilute zone of a cold pilot-scale CFB riser, by using a high-speed imaging system. The recording rate of the high-speed digital camera is as high as 5000 fps with a resolution of 640 × 480. A large number of particle movement images at a height of 3.54 m above the distributor plates were taken. Manual inspection and automatic methods based on digital image processing algorithms were carried out to analyze particle image sequences. The experimental results show that the measured particle collision rate is proportional both to the particles' average relative translational velocity and the square of the particle number density, which coincides with the collision theory derived according to the analogy of kinetic theory of gases. But the theoretical model is found to overestimate the real collision rates, and a coefficient a of 0.33 may be used to correct this discrepancy. The possible reasons for this discrepancy are also discussed. The measurement results of collision properties based on more than 50 particle collision events agrees well with Walton's hard-sphere collision model. The three collision parameters, i.e., the average coefficient of friction μ, the normal and tangential coefficients of restitution e and β_0, for the glass beads used are measured to be 0.175 ± 0.005, 0.96 ± 0.02, and 0.43 ± 0.09, respectively.

1. Introduction

Gas–solid two-phase flows have wide applications in technical and industrial processes. Examples are pneumatic conveying, fluidized beds, particle separation in cyclones, mixing devices, and others. Interparticle collision plays an important role on the particle motion behavior as well as the evolution of gas–solid flow (Fohanno and Oesterlé, 2000; Volkov et al., 2005). However, the collision behavior is rather complicated, as it is related to the inertia properties of the particles and the turbulence properties of the flow. Relatively simple solutions to this problem may be derived with the assumption of homogeneous isotropic and stationary fluid turbulence. In fact, there exist two limiting cases for investigation of particle collision identified by the Stokes number St which is the ratio of particle response time τ_p to the characteristic time scale of turbulence T_t. One is for particles of small size compared with the Kolmogorov length scale and following the turbulence perfectly ($St \to 0$) (Saffman and Turner, 1955). The other case is $St \to \infty$, in which the particle move almost with no response to turbulence of fluid and hence the velocities of particles do not correlate with each other through the fluid (Abrahamson, 1975). The latter case is under the analogy of kinetic theory, based on which the interparticle collision rate has a statistical formula, which is a function of particle number density, ensemble relative velocity, and effective collisional diameter.

Because of the practical interest, a number of theoretical studies of the collision rate have been carried out (Abrahamson, 1975; Williams and Crane, 1983; Sommerfeld and Zivkovic, 1992; Oesterlé and Petitjean, 1993; Goldshtein and Shapiro, 1995; Kruis and Kusters, 1997; Zhou et al., 1998; Wang et al., 1998; Hu and Mei, 1998; Mei and Hu, 1999; Fan et al., 2001). Sommerfeld and Zivkovic (1992) and Oesterlé and Petitjean (1993) developed independently probabilistic interparticle collision models (particles are assumed monodispersed with a size of d_p):

$$N_c = \frac{1}{2} a \pi d_p^2 u_r N^2 \tag{1}$$

where u_r, N are the average relative velocity between particles and particle number density, respectively. a is a coefficient which equals to 1 in Sommerfeld and Zivkovic's model, while in Oesterlé and Petitjean's model, a equals to $\sqrt{2}$ accounting for the difference between the one-dimensional situation and the three-dimensional one, with the assumption of a Maxwellian distribution of the particle relative velocity with respect to the local average particle velocity.

* Corresponding author. Tel.: +86 571 87952802; fax: +86 571 87951616.
E-mail address: qhwang@cmee.zju.edu.cn (Q. Wang).

0301-9322/$ - see front matter © 2008 Published by Elsevier Ltd.
doi:10.1016/j.ijmultiphaseflow.2008.04.001

The reliability of these theoretical collision models needs to be validated by direct experimental measurements before they can be used in numerical simulations for the gas–solid flows. Unfortunately, the experimental validation work is seldom reported, due to some difficulties encountered. Recently, You et al. (2004) conducted an experiment to measure the collision rate of particles with a diameter of 1.8 mm in a special particle collision device using a high-speed camera and particle tracking velocimetry (PTV) algorithms. In this special device, all particles in the upper region are falling vertically without any interparticle collision. In the second region, some of these particles change their original trajectories by colliding with inclined side walls and then collide with other particles which keep on falling vertically. Obviously, the experiment belongs to the case of $St \to \infty$, since the particles are relatively large and of high inertia and the gas phase is initially static. The experimental expression of collision rate was found to be:

$$N_c = 2.6 \times 10^5 d_p^2 u_r N^{1.15}. \quad (2)$$

As can be seen, it showed a large discrepancy compared with the theoretical model under the analogy of kinetic theory. The most important difference is that the collision rate is proportional to $N^{1.15}$ rather than N^2, which makes the expression to be dimensionally incorrect. The reason might be that the interparticle collision in this gas-particle flow is not random and may be far away from that defined by the theoretical models and also different from an actual gas–solid flow system, e.g., the flow in the riser of a CFB. Therefore, it is necessary to carry out more experimental measurements in real gas–solid flows.

This is one of the goals of our present study, which aims to carry out direct measurements of collision rates for spherical particles in the real gas–solid flow inside a cold CFB riser. And another purpose is focused on the measurements of particle collision properties, which are concerned with the dynamics of particle collisions.

From a theoretical point of view, the collision between two inelastic frictional spheres is particularly difficult due to complicated mechanisms responsible for energy dissipation and to mechanical coupling between normal and tangential deformations. In the numerical simulations of particulate flows, interparticle collisions if considered are usually solved using prescribed force schemes for soft-sphere simulations (Tsuji et al., 1993; Mikami et al., 1998; Kawaguchi et al., 1998; Gera et al., 1998) or collision operators for hard-sphere simulations (Ouyang and Li, 1999; Hoomans et al., 1996; Goldschmidt et al., 2002). A basic requirement of numerical simulations as well as theories is that the interaction model used be sufficiently simple to guarantee numerical efficiency or allow for tractable calculations. A simple collision operator that captures the main features of the oblique collision was introduced by Walton and Braun (1986). This hard-sphere model describes the collision processes by using only three collisional properties that permit unambiguous determination of the linear and angular velocities of each particle in detail and has been thus widely used in the numerical simulations. The three properties are the coefficient of friction, the normal coefficient of restitution, and the tangential coefficient of restitution, which essentially depend on the actual nature of the colliding particles and of the experimental conditions. The only way to obtain those properties is direct experimental measurement. Although the particle-wall collision properties have been extensively measured (Fohanno and Oesterlé, 2000; Liu, 1965; Lorenz et al., 1997; Foerster et al., 1994), few studies on interparticle collisions can be found due to the complex setting of such experiments. Among those limited reports, Foerster et al. (1994) described an experimental apparatus that measures the collision properties of both soda lime glass particles with a diameter of 3.18 mm and cellulose acetate particles with a diameter of 5.99 mm. Their apparatus included a mechanism that brought two identical particles into a collision without initial spin and a stroboscopic setup that photographed the dynamics of their flights. The same experimental setup was adopted by Lorenz et al. (1997) to measure the collision properties of several kinds of nearly spherical particles including glass beads with a diameter of 2.97 mm, stainless steel particles with a diameter of 5 mm, acrylic particles with that of 4 mm and polystyrene particles with that of 4 mm as well. The only difference was that they used a Kodak DCS digital camera instead of the film camera. In both of their experiments, only positions and translational velocities of the two particles during the whole collision processes were measured, i.e., the particle rotation speeds were not measured but calculated with the conservation equation of angular momentum. And this is feasible only under the prerequisite that the rotation speeds of two particles should be zero before collision. Labous et al. (1997) used another improved particle colliding apparatus and an Ektapro 1000 high-speed video system to measure the collision properties of nylon spheres with a diameter of 25.4 mm. In experiment, the rotation speeds of particles were measured directly. These limited experimental measurements showed on one hand that the high-speed imaging system was quite suitable in the measurement of particle collision properties. But on the other hand, the particles used were normally a little bit larger than those encountered in the fields of energy and chemical engineering. Furthermore, there are no reports available on the direct measurements of collision properties for the particles in real gas–solid flows.

In this paper, attempts have been made to carry out direct measurements of collision rates as well as collision properties for those moving glass beads in a cold CFB riser. The relation between the collision rate and the particle number density is analyzed and compared with commonly used relations based on kinetic theory and the results derived from the experimental methods by other researchers. The collision properties for Walton's hard-sphere model for the glass beads are obtained by analyzing the particle collision processes. The paper is organized as follows. The experimental setup, the measurement system and particle image processing methods are described in Section 2. Section 3 presents the measurement results both for collision rate and collision properties. Conclusions are given in Section 4.

2. Materials and methods

2.1. Experimental setup

The main facilities used in the experiment include a cold pilot-scale CFB system and a high-speed digital imaging system. Fig. 1

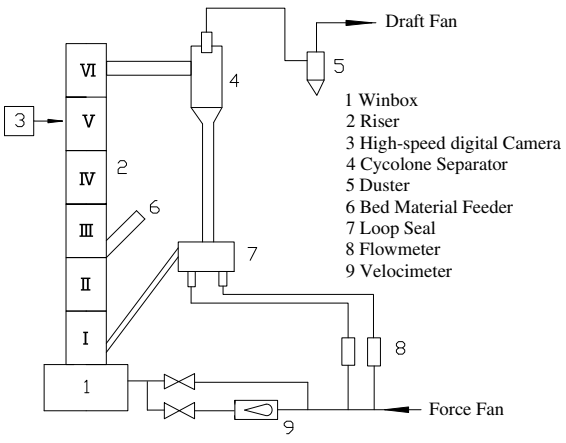

Fig. 1. System diagram of cold CFB system.

shows the system diagram of the cold CFB system, which is composed of a riser with a dimension of 200 mm × 200 mm × 4 m (H), a down pipe, a cyclone separator, a loop seal and a duster. The bed material (solid-phase) is fluidized by air which is introduced through distributor plates, and then is carried into the cyclone separator where gas-phase and solid-phase are separated. Solid-phase circulation is created when the particles go back to the riser through the loop seal. Considering the fact that there is too much high mass loading of particles in dense and transition zones, the laser sheet light is not powerful enough for penetration and the particles on images are overlapping, we have no choice but to select a cross-section area in the upper dilute-phase zone as our main measurement area. This cross-section area is 3.54 m high above the distributor plates. Spherical glass beads are used as the bed material. Their excellent optical characteristics, such as high reflectivity and high scattering efficiency ensure the quality of particles images. To minimize the effects of the shape and size of particles to the measurement results, those glass beads are with a high degree of sphericity up to 92% and are monodisperse with diameters of 500 ± 50 μm. The particle relaxation time is estimated to be much larger than the turbulence integral time scale, so the present experiment basically belongs to the case of $St \to \infty$, which is under the analogy of kinetic theory.

The high-speed digital imaging system consists of a high-speed CMOS camera, a high-power laser sheet and a computer. The camera, Redlake HG-100K, has a CMOS color sensor with a maximal recording rate of 100 kfps. In our experiment, a moderate recording rate of 5000 fps (at a resolution of 640 × 480) is used since higher recording rate is not necessary. A Nd:YAG laser with a wave length of 532 nm and a power of 8 W is used as illuminant.

2.2. Particle image acquisition

As a two-dimensional imaging apparatus, the measurement system is arranged as the same as PIV or PTV systems, as shown in Fig. 2. A vertical plane in the measurement volume is illuminated by the laser light sheet with a thickness of 4 mm, while the camera takes particle images along the direction perpendicular to the light plane. One important parameter, the camera field range needs to be tested and adjusted to meet the requirement in observing particle collisions. Normally different camera field ranges are used in the measurements of collision rate and collision properties. Since it's not necessary to know the detail collision processes in the particle collision rate study, a bigger field range, as large as 11.2 mm × 8.4 mm, is adopted. As for the measurements of collision properties, one needs to determine as accurately as possible

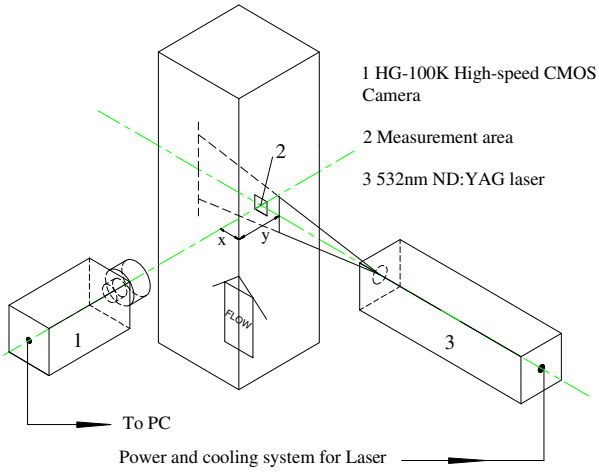

Fig. 2. Arrangement of high-speed digital imaging system.

the kinematics of the two colliding particles before and after collision. Therefore, a smaller field range is preferable. In our experimental condition, a field range of 6.7 mm × 5 mm is small enough to enable us to measure translational velocities, sizes and rotation speeds of particles before and after collisions. Examples of typical particle images obtained using these two camera field ranges are shown in Fig. 3.

The field range is kept constant during the experiment. The images of particles inside the measurement area are focused by adjusting the object distance of the camera.

2.3. Image processing methods

Several parameters concerning interparticle collision rates and collision properties are required. The collision rate is a function of particle diameter, particle number density and relative translational velocities between particles. Furthermore, the translational velocities, sizes and rotation speeds for the two colliding particles are required in the calculations of collision properties. To obtain all these parameters, manual methods may be used. But in more efficient way, some of the parameters can be obtained using digital imaging processing techniques.

The *particle translational velocity* can be calculated by the well known PTV techniques (Adrian, 1996; Yamamoto et al., 1996; Ishikawa and Yamamoto, 1997; Guezennee et al., 1994; Kasagi and Nishino, 1991; Nishino et al., 1991). A spring-model algorithm is used to obtain translational velocity for each particle in the images here as recommended by You et al. (2004).

The *average relative translational velocity* is based on the translational velocities of all particles in the measurement volume for a period of time and can be obtained by the following expression:

$$u_r = \frac{1}{N_t}\sum_{k=1}^{N_t}\left[\frac{1}{(N_p-1)N_p}\sum_{i=1}^{N_p}\sum_{\substack{j=1\\ j\neq i}}^{N_p}|\mathbf{u}_i-\mathbf{u}_j|\right] \tag{3}$$

where N_p is the total number of particles in the investigation volume, N_t is the number of frames used for analysis, $|\mathbf{u}_i - \mathbf{u}_j|$ is the relative velocity of two particles in the investigation volume.

The sizes of glass beads are monodisperse with 500 ± 50 μm in diameter provided by the manufacture. However, the particle images contain more accurate size information. The edge detection method can be used in the *particle size* measurements based on which the *average particle size* is given by:

$$d_p = \frac{1}{N_t}\sum_{k=1}^{N_t}\left[\frac{1}{N_p}\sum_{i=1}^{N_p} d_i\right] \tag{4}$$

The *particle number density* is the particle number per unit volume, which is defined as

$$N = \frac{1}{N_t}\sum_{k=1}^{N_t}\frac{N_p}{\Delta V}. \tag{5}$$

N_p can be obtained automatically by counting the number of particles in the field range by a program which is already involved in the PTV algorithm. The investigation volume ΔV is determined by the camera field range and the depth of focus. The latter may be regarded as the depth of the laser light sheet, which is about 4 mm in our experiment.

The *collision rate* N_c is defined as the total collision number per unit time per unit volume. The collision event is counted manually when the particle image sequences are observed one by one. Together with the investigation volume ΔV and the time interval Δt, the collision rate turns out to be:

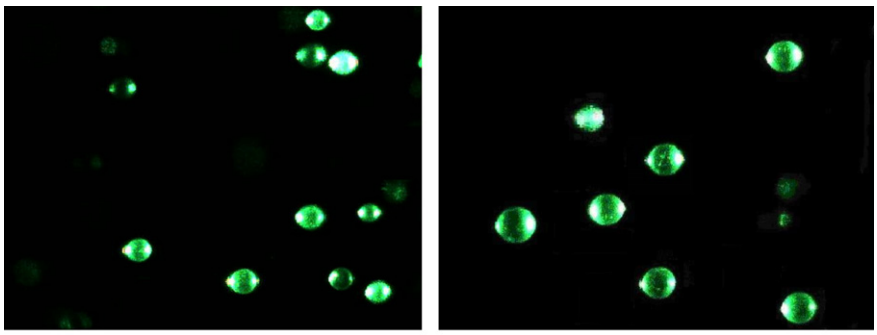

Fig. 3. Raw images taken by using different camera field ranges. Height of bed materials: 400 mm, superficial gas velocity: 5 m/s, external solids mass flux: 1.5 kg m^{-2} s^{-1}, particle average diameter: 0.5 mm.

$$N_c = \frac{C}{\Delta V \Delta t}. \tag{6}$$

where C is the total collision number in the investigation volume for the time interval Δt.

The *particle rotation speed* is measured manually. As the glass beads are normally not ideal spheres with smooth surfaces, some speckles on their surfaces may be recognized (for example, particles shown in Fig. 7) under the illumination of laser light. When the particle rotates, the position of these speckles changes, based on which the rotation angle of the particle may be determined. The particle rotation speed is the rotation angle divided by the time interval. The detail information about the manual method has been introduced elsewhere (Wu et al., 2008).

3. Result and analysis

3.1. Collision rate

The cold CFB is operated at a basic condition with a superficial gas velocity of 5 m/s (the corresponding Reynolds number is 6.34×10^4, neglecting the presence of the particles), external solids mass flux of 1.5 kg/(m^2 s) and the height of bed materials of 400 mm. Examples of typical raw particle collision events are in "collision1.gif" and "collision2.gif" files. During the experiment, the operation parameters are adjusted to change the flow condition, i.e., with different particle number densities and different average relative translational velocities. For each working condition, more than 50,000 particle images have been taken at the measurement point 80 mm (y) and 50 mm (x) away from the riser sides in directions towards the camera and the laser, among which about 1000 images extracted randomly were used to calculate the average data of particle number density and relative velocity by the imaging processing program, while total images are browsed to counter the total collision number and collision rate. It is assumed that the particle collision rate is proportional to the square of particle size and has an expression similar to the Eq. (1), since the present experiment basically belongs to the case of $St \to \infty$:

$$N_c = \left[\frac{1}{2} a\pi d_p^2\right] \cdot u_r^A \cdot N^B \tag{7}$$

but here a, A, B instead of 1 (or$\sqrt{2}$), 1, 2, are the underdetermined coefficients. By changing the working condition, a group of data $\{u_r, N, N_c\}$ is obtained. The variation ranges of u_r and N are 0.05–0.5 m/s (the average particle velocity is in the range of 0.5–1 m/s) and 5–65 cm^{-3}.

If we define three new variables, $y = \log(N_c)$, $x_1 = \log(u_r)$, $x_2 = \log(N)$, Eq. (7) becomes a bivariate linear equation:

$$y(x_1, x_2) = C + Ax_1 + Bx_2 \tag{8}$$

where $C = \log\left[\frac{1}{2} a\pi d_p^2\right]$, and a is another underdetermined coefficient. The group of data $\{y, x_1, x_2\}$ is then analyzed by the binary linear regression method. As shown in Fig. 4, the linear regression plane (grid plane) is well fitted from the data group of spatial points, with a regression coefficient R^2 up to 0.99. Three underdetermined coefficients a, A, B turn out to be 0.349, 1.0112 and 1.9923, respectively. The final expression is:

$$N_c = \frac{1}{2} a\pi d_p^2 u_r^{1.0112} N^{1.9923} \tag{9}$$

where $a = 0.35$. That is to say, the particle collision rate is essentially proportional both to the relative velocity and the square of particle number density, which is dimensionally correct and in accord with the theoretical result. Nevertheless, the coefficient a is much lower. It seems that the theoretical results based on kinetic theory of gases overestimate the actual collision rates of particles in a real CFB riser. Fig. 5 compares the particle collision rates at different particle number densities based on our results and other reported expressions, with particle size and relative velocity of 500 μm and 0.1 m/s, respectively.

Note that the reliability of this conclusion may be affected by measurement errors. Several parameters, i.e., the average particle diameter, particle numbers, the investigation volume, the total col-

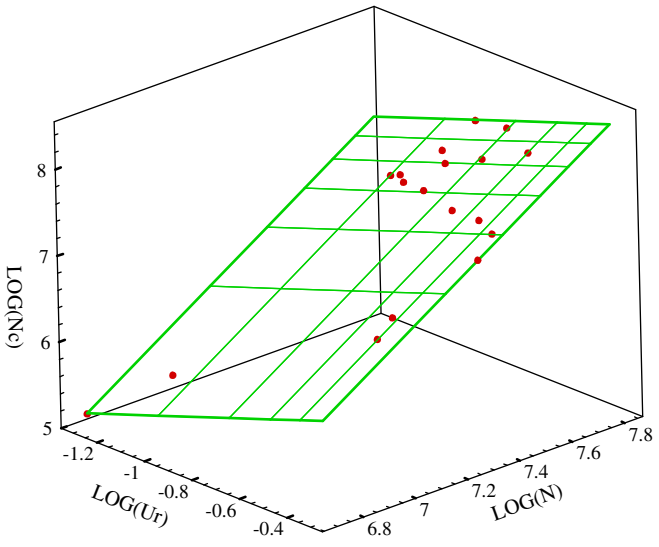

Point: experimental data; gridplane: linear regression result

Fig. 4. Linear regression analysis of experimental data of particle collision rate as a function of relative translational velocity and particle number density, $\mathrm{Log}(N_c) = -C + A\mathrm{Log}(u_r) + B\mathrm{Log}(N)$, $C = -6.8631$, $A = 1.0112$, $B = 1.9923$, $R^2 = 0.9907$.

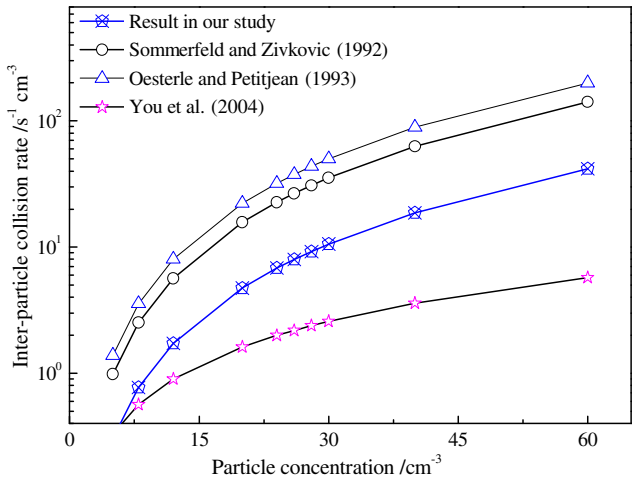

Fig. 5. Comparison of Inter-particle collision rates obtained by experiments and theoretical analyses as a function of particle number density, d_p = 500 μm, u_r = 0.1 m/s.

lision numbers as well as the average relative translational velocity are measured experimentally. Among them, the investigation volume is the product of camera field range area and the depth of focus perpendicular to the field range plane. In fact, the depth of the investigation volume is considered to be the width of the laser light sheet, which is smaller than the real one, as indicated by You et al. (2004). Their correction method is employed and the results turn out to be 4.25 mm. Considering this factor, the original particle number density as well as the collision rate may be revised by multiplying with a coefficient of 16/17, which leads to the coefficient a to be corrected by a factor of 17/16. The average relative translational velocity obtained based on translational velocity of each particle is also lower than the real one due to the fact that the gas–solid flow is three-dimensional rather than two-dimensional. The experimental measurement system as well as the PTV calculation program neglected the particle's third velocity component perpendicular to the light sheet plane. To consider this issue, the positions of the camera and the laser are exchanged so that the third velocity component can be measured. Since the three velocity components (two horizontal (x, y) and one vertical) can not be measured at the same time, only average velocity based on a large number of particle samples under various working conditions is considered. It is found that the three average velocity components are 0.72 m/s (vertical direction), 0.43 m/s (x-direction) and 0.33 (y-direction). Thus a fact of 0.93 is needed to correct the coefficient a. The size of glass beads provided by the manufactory may be not accurate enough and the deviation may also affect the value of the coefficient a. So a large number particle images have been used to analyze the size information of glass beads by using digital image processing methods. The result shows that the glass beads have sizes of 508.7 ± 55 μm based on more than 10,000 particles. The deviation of particle size leads to the coefficient a to be corrected by a factor of $(500/508.7)^2$. It can be seen that with there factors in consideration, the final value of the coefficient a may be 0.33, which is only 23.6% of the value in the theoretical model.

The discrepancy between the experimental and theoretical values of the coefficient a need to be further discussed. According to the experimental condition, the particle relaxation time and the turbulence integral time scale are about 1.88 s and 0.04 s, separately, which yield the Stokes number St to be 47. So it basically belongs to but does not reach the limit case of $St \to \infty$. Direct numerical simulation of interparticle collisions in isotropic turbulence by Li et al. (2006) suggested that the kinetic theory ($St \to \infty$) would overestimate the collision rate for finite-inertia particle (finite Stokes number). According to their simulation result, the predicted collision rate in our experimental condition is about 70% of that obtained by the kinetic theory. This might be one of the reasons for the discrepancy of the coefficient a. Another reason is probably due to the different flow condition between the present gas solid flow and the ideal flow defined in the kinetic theory. For the latter, a stationary isotropic homogeneous turbulent flow is assumed. Meanwhile, particles in the flow are statistically independent, i.e., their relative motion is completely uncorrelated and similar to the chaotic motion of molecules. However, the flow in the real cold CFB riser is neither stationary nor isotropic homogeneous turbulent, and the motion behavior of particles has essentially different characteristic from that of the gas molecular, since they are dominated not only by collisions but also by the forces exerted on them, such as gravitational force, drag force by the flow, etc. The forces may have influences that lead to the motion of particles to be more deterministic other than stochastic, which reduce the probability of particle collision behavior.

3.2. Collision property

This section describes the measurement results of the collision properties for spherical glass beads. The measured collision properties are relevant to the so called hard-sphere model introduced by Walton and Braun (1986) which is also briefly recalled here.

3.2.1. Definition of collision properties

Let us consider two homogeneous spherical particles with masses m_1 and m_2, diameters d_1 and d_2, moments of inertia about their center I_1 and I_2. Prior to the collision the particle centers have translational velocities $\mathbf{u}_1$ and $\mathbf{u}_2$ and angular velocities $\boldsymbol{\omega}_1$ and $\boldsymbol{\omega}_2$. During the collision sphere 2 exerts an impulse $\Delta\mathbf{P}$ on sphere 1, as shown in Fig. 6. The new values of two kinds of velocities hereafter denoted with a prime, are obtained from the conservation of linear momentum,

$$\Delta\mathbf{P} = m_1(\mathbf{u}_1' - \mathbf{u}_1) = m_2(\mathbf{u}_2 - \mathbf{u}_2') \tag{10}$$

of angular momentum,

$$-\mathbf{n} \times \Delta\mathbf{P} = \frac{2I_1}{d_1}(\boldsymbol{\omega}_1' - \boldsymbol{\omega}_1) = \frac{2I_2}{d_2}(\boldsymbol{\omega}_2 - \boldsymbol{\omega}_2') \tag{11}$$

and from prescribed relations using the collision properties. In Eq. (11) $\mathbf{n}$ is the unit vector joining the centers of the two particles. The normal coefficient of restitution e is defined as

$$e = -\frac{(\mathbf{u}_1' - \mathbf{u}_2') \cdot \mathbf{n}}{(\mathbf{u}_1 - \mathbf{u}_2) \cdot \mathbf{n}} \tag{12}$$

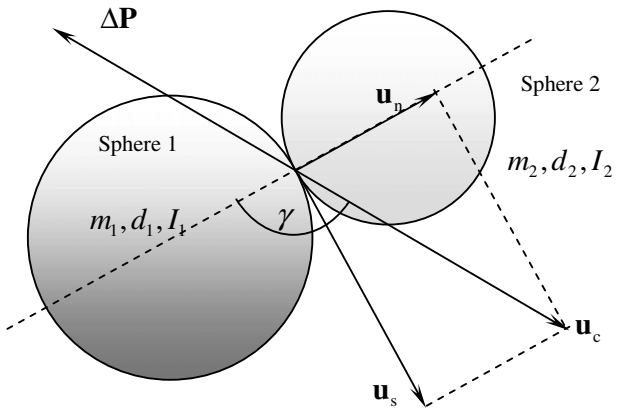

Fig. 6. Relative kinematics of two colliding spherical particles.

It is a measure of the energy lost in the normal direction of the relative impact motion. The relative velocity of the particles at their contact point before collision is (see Fig. 6)

$$\mathbf{u}_c = \mathbf{u}_1 - \mathbf{u}_2 - 1/2(d_1\omega_1 + d_2\omega_2) \times \mathbf{n}. \quad (13)$$

The tangential component of u_c is defined as u_s, which introduces the definition of the tangential coefficient of restitution β

$$\mathbf{u}_s' = -\beta \mathbf{u}_s \quad (14)$$

Note that the direction of u_s is assumed to be unchanged but its modulus is reduced by a factor $|\beta|$. The tangential coefficient of restitution β is not a constant however, due to the different collision condition throughout the contact point, i.e., sliding or rolling which is a function of the angle of incidence γ. A critical angle of incidence γ_0 is introduced for the judgement and β is given according to the following equation,

$$\beta = \begin{cases} -1 - 3.5\mu(1+e)\frac{u_n}{u_s} & \text{for} \quad \gamma \leqslant \gamma_0 \quad \text{(sliding)} \\ \beta_0 & \text{for} \quad \gamma > \gamma_0 \quad \text{(rolling)} \end{cases} \quad (15)$$

where β_0 is the value of tangential coefficient of restitution for rolling collision. According to the Eq. (15), the two parameters, i.e., μ and β_0, can be determined by producing a plot of β values versus $-u_n/u_s$.

As can be seen, the linear and angular velocities of two colliding particles after collision can be determined unambiguously if both the collision properties, i.e., μ, e and β_0 and particles' motion parameters before collision are known.

3.2.2. Collision properties

It is mentioned that the gas–solid flow inside the CFB riser is three-dimensional rather than two-dimensional. The particle trajectories as well as particle collisions may also be in arbitrary directions in the flow space. Therefore, it poses a big challenge to measure the motion parameters, including translational velocities and rotation speeds, of the two colliding particles before and after collision, by using our two-dimensional high-speed digital imaging system. The latter, i.e., particle rotation speed, is far more difficult to measure than the former, as indicated by Lorenz et al. (1997). Fortunately, measurements of rotation speeds for spherical glass beads in such a gas–solid flow have already been investigated and the measurement method as well as some preliminary experimental results was published elsewhere (Wu et al., 2008).

The motion parameters need to be measured as accurately as possible, so that the collision properties obtained are of high reliability. Since the two-dimensional high-speed digital imaging system is only capable of measuring the particle's translational velocity components in the object plane rather than the real three-dimensional velocity, the particle collision cases used for collision property analysis are filtered out among all the collision events observed in the experiment and the following conditions should be satisfied:

(1) the two colliding particles are (nearly) spherical;
(2) the collision process and the trajectories of two particles before and after collision are in the laser light sheet plane, so that the third translational velocity component perpendicular to the light sheet plane is indistinctive and may be neglected;
(3) the rotation speeds of two particles may be measured.

Note that the majority of the particle collision events observed does not coincide with these three conditions, and therefore, it's necessary to take a large number of particle images in the experiment and one need to be patient enough to find this kind of collision events by browsing particle image sequences. The work is very tedious, by the way. The total number of particle images amounts to 500,000 and about 50 collision events satisfying the above conditions are obtained. A typical example is shown in Fig. 7.

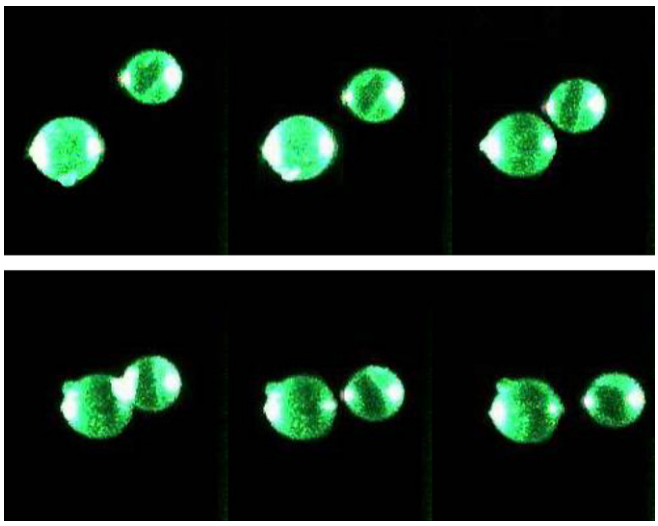

Fig. 7. Sequence of images for a particle collision process.

By analyzing all these collision events, the interparticle collision properties for the glass beads, i.e., the coefficient of friction μ, the normal coefficient of restitution e, and the tangential coefficient of restitution β_0, can be achieved. The normal coefficient of restitution is found to be about 0.96 ± 0.02. Fig. 8 shows the coefficient of tangential restitution versus the cotangent of the angle of incidence, $-u_n/u_s$. By linear fitting method, two lines are obtained from which we observe the qualitative behavior predicted by Walton's model (see Eq. (15)): for low values of $-u_n/u_s$, β first increases linearly until it reaches a maximum positive value $\beta_0 = 0.43 \pm 0.09$. From the slope of this fitting line we can extract the coefficient of friction $\mu = 0.175 \pm 0.005$. All the values of the collision properties obtained are very close to those measured by other researchers for relative larger particles (Foerster et al., 1994; Lorenz et al., 1997; Labous et al., 1997; Kharaz et al., 1999). The experimental results show on the other hand that the Walton's model based on three constant coefficients captures the behavior of interparticle

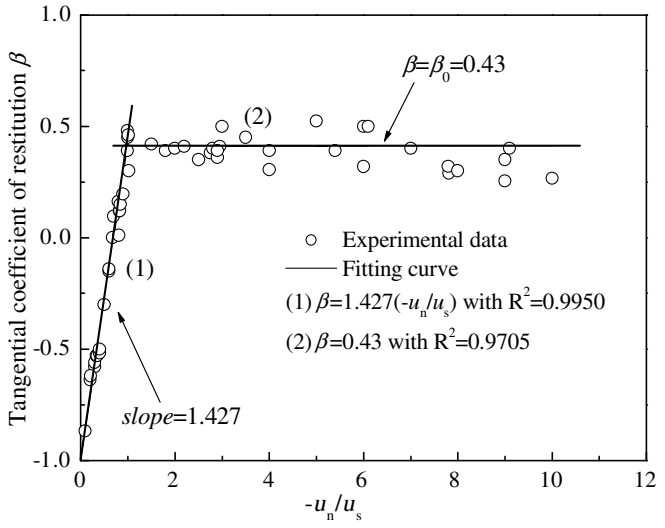

Fig. 8. Coefficient of tangential restitution vs the cotangent of the angle of incidence.

collisions of glass beads used in the experiments in the cold CFB riser and therefore this simple model is proved to be reasonable and reliable in our case. The main uncertainties in determination of collision properties are the values and directions of the particle velocities, and the shape of particles. To perform more accurate measurement of particle collision properties, one needs to develop flow visualization and velocity measurement in three dimensions and to use particles with higher sphericity.

4. Conclusion

By using a high-speed digital imaging system, interparticle collisions of glass beads with an average diameter of 0.5 mm in the upper dilute phase zone of a cold pilot-scale CFB riser have been investigated experimentally. Two aspects were focused on, i.e., the collision rates and collision properties measurements.

It is shown that the particle collision rate is likely to be proportional both to the particles' average translational velocity and the square of the particle number density, which coincide with the theoretical results derived from the analogy of kinetic theory of gases. But the theoretical model is found to overestimate the real collision rates in the real gas–solid two-phase flow, and a coefficient a of 0.33 may be used to correct this discrepancy. The possible reasons for this discrepancy may probably be the differences between the real gas–solid flow and the ideal one defined by the kinetic theory, including the finite Stokes number, the status of the flow, and the status of the particles. The measurement results of collision properties agrees well with the Walton's hard-sphere collision model and the three collision parameters, i.e., the average coefficient of friction μ, the normal and tangential coefficients of restitution e and β_0, for the glass beads used are measured to be with values of 0.175 ± 0.005, 0.96 ± 0.02, and 0.43 ± 0.09, respectively, which are very close to those measured by other researchers for relative larger particles.

Acknowledgements

The authors gratefully acknowledge the financial supports from the National Eleven-five Year Key Technology R&D program under Grant No. 2006BAA03B01 and the China Postdoctoral Science Foundation funded project under Grant No. 20070421165.

Appendix A. Supplementary material

Supplementary data associated with this article can be found in the online version, at doi:10.1016/j.ijmultiphaseflow.2008.04.001.

References

Abrahamson, J., 1975. Collision rates of small particles in a vigorously turbulent fluid. Chem. Eng. Sci. 30, 1371–1379.
Adrian, R.J., 1996. Bibliography of Particle Velocimetry Using Imaging Methods. University of Illinois at Urbana-Champaign, p. 5.
Fan, J.R., Yao, J., Zhang, Y.X., Cen, K.F., 2001. Modeling particle-to-particle interactions in gas–solid flows. J. Eng. Thermophys. 22, 629–632 (in Chinese).
Foerster, S.F., Louge, M.Y., Chang, H., Allia, K., 1994. Measurements of the collision properties of small spheres. Phys. Fluids 6, 1108–1115.
Fohanno, S., Oesterlé, B., 2000. Analysis of the effect of collisions on the gravitational motion of large particles in a vertical duct. Int. J. Multiphase Flow 26, 267–292.
Gera, D., Gautam, M., Tsuji, Y., Kawaguchi, T., Tanaka, T., 1998. Computer simulation of bubbles in large-particle fluidized beds. Powder Technol. 98, 38–47.
Goldschmidt, M.J.V., Beetstra, R., Kuipers, J.A.M., 2002. Hydrodynamic modelling of dense gas-fluidised beds: comparison of the kinetic theory of granular flow with 3D hard-sphere discrete particle simulations. Chem. Eng. Sci. 57, 2059–2075.
Goldshtein, A., Shapiro, M., 1995. Mechanics of collisional motion of granular materials. Part 1: general hydrodynamic equations. J. Fluid Mech. 282, 75–114.
Guezennee, Y.G., Brodkey, R.S., Trigui, N., Kent, J.C., 1994. Algorithm for fully automated three-dimensional particle tracking velocimetry. Exp. Fluids 17, 209–219.
Hoomans, B.P.B., Kuipers, J.A.M., Briels, W.J., Van Swaaij, W.P.M., 1996. Discrete particle simulation of bubble and slug formation in a two-dimensional gas-fluidised bed: a hard-sphere approach. Chem. Eng. Sci. 51, 99–118.
Hu, K.C., Mei, R., 1998. Particle collision rate in fluid flows. Phys. Fluids 10, 1028–1030.
Ishikawa, M., Yamamoto, F., 1997. A novel PIV system using parallel processing of flow analysis and image analysis. In: Proceedings of International Conference on Fluid Engineering, pp. 657–662.
Kasagi, N., Nishino, N., 1991. Probing turbulence with three-dimensional particle tracking velocimetry. Exp. Therm. Fluid Sci. 4, 601–612.
Kawaguchi, T., Tanaka, T., Tsuji, Y., 1998. Numerical simulation of two-dimensional fluidized beds using the discrete element method (comparison between the two- and three-dimensional models). Powder Technol. 96, 129–138.
Kharaz, A.H., Gorham, D.A., Salman, A.D., 1999. Accurate measurement of particle impact parameters. Meas. Sci. Technol. 10, 31–35.
Kruis, F.E., Kusters, K.A., 1997. The collision rate of particles in turbulent flow. Chem. Eng. Commun. 158, 201–230.
Labous, L., Rosato, A.D., Dave, R.N., 1997. Measurements of collisional properties of spheres using high-speed video analysis. Phys. Rev. E 56, 5717.
Li, R., Liu, Z., He, Z., Chen, Y., Zhengzhou, C., 2006. Direct numerical simulation of inerttial particle collisions in isotropic turbulence. Chin. J. Theor. Appl. Mech. 38, 25–32.
Liu, H.X., 1965. Discussion on movement regularity of solid fuel in a cyclone furnace. In: Engery Department. Zhejiang University, Hangzhou.
Lorenz, A., Tuozzolo, C., Louge, M.Y., 1997. Measurements of impact properties of small, nearly spherical particles. Exp. Mech. 37, 292–298.
Mei, R., Hu, K.C., 1999. On the collision rate of small particles in turbulent flows. J. Fluid Mech. 391, 67–89.
Mikami, T., Kamiya, H., Horio, M., 1998. Numerical simulation of cohesive powder behavior in a fluidized bed. Chem. Eng. Sci. 53, 1927–1940.
Nishino, N., Kasagi, N., Hirata, M., 1991. Three-dimensional particle tracking velocimetry based on automated digital image processing. J. Fluid Sci. 4, 601–612.
Oesterlé, B., Petitjean, A., 1993. Simulation of particle-to-particle interactions in gas solid flows. Int. J. Multiphase Flow 19, 199–211.
Ouyang, J., Li, J., 1999. Particle-motion-resolved discrete model for simulating gas–solid fluidization. Chem. Eng. Sci. 54, 2077–2083.
Sommerfeld, M., Zivkovic, G., 1992. Recent advances in the numerical simulation of pneumatic conveying through pipe system. In: HIRSCH (Ed.), Computational Methods in Applied Science First European Computational Fluid Dynamics, Brussels, pp. 201–212.
Saffman, P.G., Turner, J.S., 1955. On the collision of drops in turbulent clouds. J. Fluid Mech. 1, 16–30.
Tsuji, Y., Kawaguchi, T., Tanaka, T., 1993. Discrete particle simulation of two-dimensional fluidized bed. Powder Technol. 77, 79–87.
Volkov, A.N., Tsirkunov, Y.M., Oesterle, B., 2005. Numerical simulation of a supersonic gas–solid flow over a blunt body: the role of inter-particle collisions and two-way coupling effects. Int. J. Multiphase Flow 31, 1244–1275.
Walton, O.R., Braun, R.L., 1986. Viscosity, granular-temperature,and stress calculations for shearing assemblies of inelastic, frictional disks. J. Rheol. 30, 949–980.
Wang, L.-P., Wexler, A.S., Zhou, Y., 1998. On the collision rate of small particles in isotropic turbulence. I. Zero-inertia case. Phys. Fluids 10, 266–276.
Williams, J.J.E., Crane, R.I., 1983. Particle collision rate in turbulent flow. Int. J. Multiphase Flow 9, 421–435.
Wu, X.C., Wang, Q.H., Luo, Z.Y., Fang, M.X., Cen, K.F., 2008. Experimental study of particle rotation characteristics with high-speed digital imaging system. Powder Technol. 181, 21–30.
Yamamoto, F., Wada, A., Iguchi, M., Ishikawa, M., 1996. Discussion of the cross-correlation methods for PIV. J. Flow Visual. Image Process 3, 65–78.
You, C., Zhao, H., Cai, Y., Qi, H., Xu, X., 2004. Experimental investigation of interparticle collision rate in particulate flow. Int. J. Multiphase Flow 30, 1121–1138.
Zhou, Y., Wexler, A.S., Wang, L.-P., 1998. On the collision rate of small particles in isotropic turbulence. II. Finite inertia case. Phys. Fluids 10, 1206–1216.